INTERNAL TRANSPORT BARRIERS IN ALCATOR C-MOD

C. L. FIORE,* D. R. ERNST, J. E. RICE, K. ZHUROVICH, N. BASSE,† P. T. BONOLI, M. J. GREENWALD, E. S. MARMAR, and S. J. WUKITCH *Massachusetts Institute of Technology Plasma Science and Fusion Center, Cambridge, Massachusetts 02139*

Received August 10, 2005
Accepted for Publication April 20, 2006

Internal transport barriers (ITBs) marked by steep density and pressure profiles and reduction of core transport are obtained in Alcator C-Mod. Transient single barriers are observed at the back-transition from H- to L-mode and also when pellet injection is accompanied by ion cyclotron resonance frequency (ICRF) power. Double barriers are induced with injection of off-axis ICRF power deposition. These also arise spontaneously in ohmic H-mode plasmas when the H-mode lasts for several energy confinement times. C-Mod provides a unique platform for studying such discharges: The ions and electrons are tightly coupled by collisions with $T_i/T_e = 1$, and the plasma has no internal particle or momentum sources. ITB plasmas with average pressure greater than 1 atm have been obtained. To form an ITB, particle and thermal flux are reduced in the barrier region, allowing the neoclassical pinch to peak the density while maintaining the central temperature. Gyrokinetic simulation suggests that long-wavelength drift wave turbulence in the core is marginally stable at the ITB onset, but steepening of the density profile destabilizes trapped electron modes (TEMs) inside the barrier. The TEM ultimately drives sufficient outgoing particle flux to balance the inward pinch and halt further density rise, which allows control of particle and impurity peaking.

KEYWORDS: *internal transport barriers, tokamaks, Alcator C-Mod*

I. INTRODUCTION

Transport barriers that provide regions of reduced energy, particle, and/or momentum transport have been observed in a large number of toroidal plasma experiments throughout the world. The edge transport barrier that gives rise to the enhanced confinement regime known as H-mode[1] is ubiquitous in toroidal plasmas and forms the benchmark for optimized plasma performance. Transport barriers often occur in the plasma interior as well, usually under very specific operational conditions. An early observation of a particle transport barrier accompanied by improved energy confinement was found with pellet injection on Alcator C (Ref. 2). Most commonly, transport barriers in the plasma interior are found in neutral beam–heated plasmas,[3–7] where the beam provides a source of particles and momentum to the plasma. The resulting rotation of the plasma is thought to generate sufficient electromagnetic shear to stabilize ion temperature gradient (ITG)–driven instability by increasing the $E \times B$ shearing rate above its maximum linear growth rate. Other techniques use radio frequency waves to alter the internal magnetic configuration of the plasma to obtain magnetic shear stabilization of such instabilities. These include lower hybrid current drive,[8,9] ion Bernstein wave injection,[10] and electron cyclotron heating.[11] A comprehensive review of the internal transport barrier (ITB) experiments and analysis can be found in recent papers by Wolf[12] and Connor et al.[13]

The presence of ITBs has been noted under a number of different operational regimes in Alcator C-Mod (Refs. 14 through 20). They are most notable in the plasma density profile that displays strong peaking with a distinctive break in the profile near the plasma half-radius, indicating that a strong barrier to particle transport has formed. The pressure profile also displays strong gradients, which implies that no loss in thermal energy is occurring as the core density rises, indicating that a thermal barrier exists in the plasma interior as well. ITBs in Alcator C-Mod are distinguished from those reported in many other experiments in that they occur without the addition of external particle and momentum sources. Also, they most often appear in plasmas that have monotonic q profiles with $q_{\min} < 1$ and moderate magnetic shear.

In this paper, we review the experimental observations of ITBs in Alcator C-Mod that are established by

*E-mail: fiore@psfc.mit.edu
†Current address: ABB Switzerland Ltd., Corporate Research, Segelhofstrasse 1, CH-5405 Baden-Dättwil, Switzerland

such means as off-axis ion cyclotron resonance frequency (ICRF) heating (Sec. II.A), spontaneous ohmic H-modes (Sec. II.B), and pellet injection (Sec. II.C) and during H- to L-mode back-transitions (Sec. II.D). Control of these ITBs is reviewed in Sec. III, while transport analysis is presented in Sec. IV. A discussion of gyrokinetic simulations of the stability of the C-Mod ITBs is presented in Sec. V, followed by concluding remarks in Sec. VI.

II. ALCATOR C-MOD ITBs

II.A Off-Axis ICRF

Steady-state ITBs, lasting 10 or more energy confinement times, are often seen in Alcator C-Mod plasmas. These occur when long-lived enhanced D_α (EDA) H-modes are established in which the net central power is not peaked on-axis. This is common in H-mode plasmas that have been formed when ICRF power is injected into the plasma with the resonance location placed off-axis, on either the low- or high-field side of the plasma. The best results are obtained with the resonance position located at or slightly greater than $r/a = 0.5$. An example of a typical ITB density profile is shown in Fig. 1. The electron density n_e is derived from the profile of the visible bremsstrahlung radiation,[21] which has been corrected for the small contribution of $T_e^{-1/2}$, leaving $V_b = n_e^2 * Z_{eff}$. Z_{eff} is the average charge state of the plasma and is between 1 and 2 for most Alcator C-Mod plasmas. The visible bremsstrahlung data are used for presentation and analysis of the ITBs in this paper because they provide greater spatial resolution than Thomson scattering on C-Mod (208 chords compared to 6 to 8 channels) as well as better data frequency (1 kHz versus 30 Hz). Comparison of density derived from V_b to the density obtained from Thomson scattering in this case indicates that in most cases Z_{eff} has a flat radial profile, typical for most C-Mod operation. The exception occurs late in the life of an ITB when some impurities begin to accumulate in the core, often triggering a disruption or a collapse of the H-mode. A calculation of the ICRF power deposition profile is also included in Fig. 1. Note that the ITB foot position falls well inside the ICRF power peak and is clearly separate from it. As noted, Z_{eff} becomes somewhat centrally peaked late in time when a strong ITB is present. This is shown in Fig 2. Central Z_{eff} ultimately reaches a value of 3.0 late in the ITB phase of the discharge, just before the H-mode undergoes a back-transition to L-mode.

Alcator C-Mod H-mode plasmas demonstrate strong cogoing central plasma rotation. The magnitude of the velocity has been shown to be dependent upon the plasma

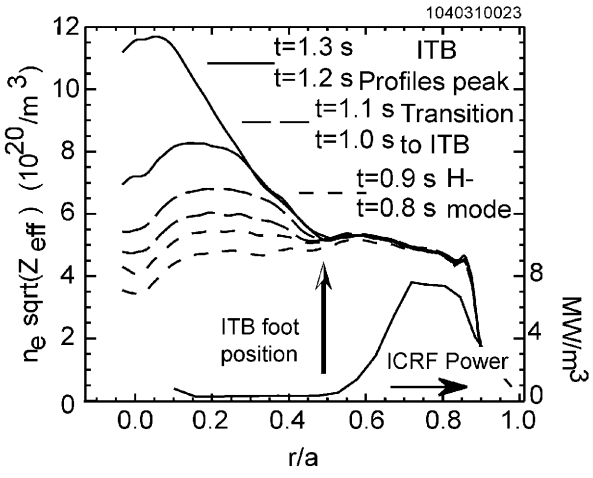

Fig. 1. Profiles of the square root of the visible bremsstrahlung emission are shown during an ITB formed with off-axis ICRF heating. A calculation of the rf deposition profile is included for comparison.

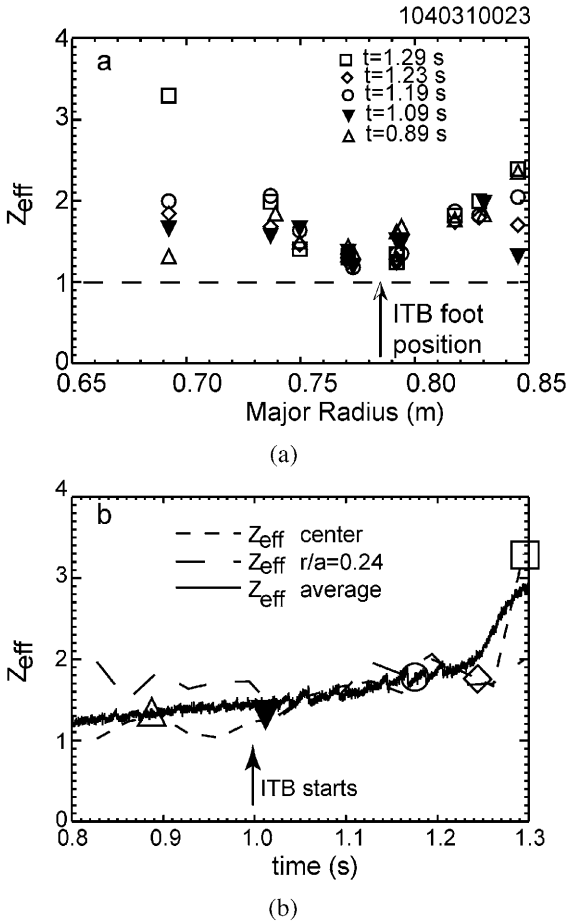

Fig. 2. Z_{eff} derived from obtaining the ratio of the square root of the visible bremsstrahlung emission to the density from Thomson scattering, shown as a function of (a) position and (b) time.

stored energy and the current.[22] It has been widely reported that this cogoing rotation slows and reverses to the counter direction as a typical ITB develops in these plasmas.[14,16,18] An example of the rotation velocity is compared for two similar discharges in Fig. 3. In both cases ICRF power of 3 MW is turned on at $t = 0.7$ s, and the plasma enters into H-mode almost immediately. In the case represented by the dashed line, the toroidal field was 4.9 T and the rf resonant layer was slightly off-axis on the high-field side. The ratio of central electron density to that from one of the outer channels from the same shot shows no peaking throughout the H-mode phase of the plasma. The solid trace in both figures is from a plasma with the same conditions, except that the toroidal field was at 4.5 T, bringing the rf resonance layer to $r/a = 0.5$, in the region where the ITB is typically formed in the Alcator C-Mod core. As can be easily seen, the rotation started to rise when the ICRF power was turned on at 0.7 s, and then it began to decrease monotonically 0.2 s later. Shortly thereafter, the density peaking factor increases, indicating that an ITB has formed. In ITBs formed at high field with high ICRF input power, the rotation decreases as the ITB forms, but it does not reverse.[20]

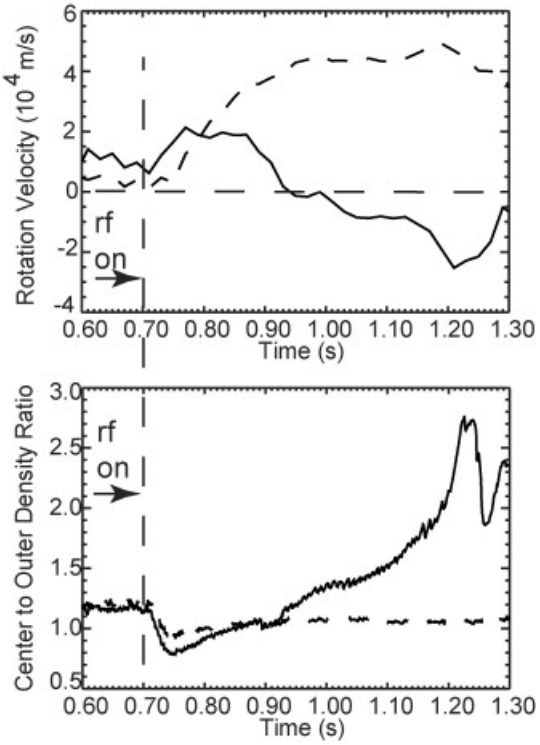

Fig. 3. The rotation velocity is compared for a standard H-mode (dashed line) with a plasma that develops an ITB (solid line), as is seen from the peaking of the density profile obtained from visible bremmstrahlung data. The ICRF power is turned on at $t = 0.7$ s and remains on throughout. The rf power is peaked on-center for the standard H-mode and at $r/a = 0.5$ for the ITB plasma.

The formation of the ITB is extremely sensitive to the applied toroidal magnetic field, suggesting that the location of the ICRF resonance position is critical for an ITB to arise. In Fig. 4, the toroidal field is scanned such that the resonance position for the 70-MHz ICRF power moves from $r/a > 0.5$ on the high-field side to $r/a > 0.5$ on the low-field side. As indicated by the peaking factor and the value of the central toroidal rotation, ITBs form when the resonance position reaches the extreme values on either side of the plasma. Other experiments suggest that changes in the applied magnetic field of even less than 1% can influence whether or not an ITB is formed. First, an H-mode is established using off-axis ICRF power at a toroidal magnetic field value that locates the ICRF resonance too close to the center for ITB development. In a subsequent experiment, the toroidal magnetic field is then ramped down, which moves the resonance farther toward the high-field side of the plasma, effectively to larger r/a position, until an ITB is produced. The converse is also done, in which an ITB is established in an off-axis ICRF-heated plasma with the magnetic field ramping up until the ITB profile is lost. Since the location of the ICRF power deposition is changed with the magnetic field ramp, it seems reasonable to suggest that the most important factor in this test is the relative amount of power located inside/outside the ITB radius. The total of the ohmic and ICRF power distribution (calculated with TRANSP using the TORIC code[23] coupled to a Fokker-Planck solver) in these plasmas is shown in Fig. 5. The ITB forms in these experiments when the power inside the ITB radius is roughly less than 40% of the total input, and the ITB terminates when the power inside the ITB radius exceeds 60% of the total.

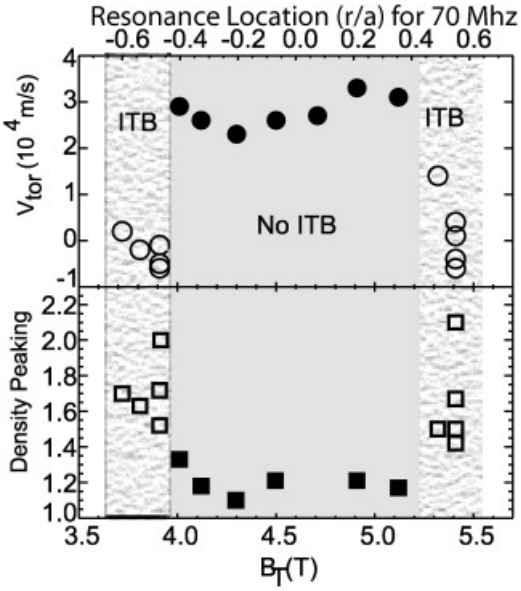

Fig. 4. Central plasma rotation and density peaking factor for a toroidal field scan with 70-MHz ICRF power.

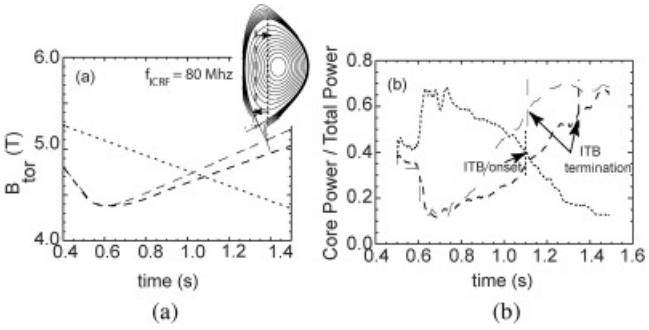

Fig. 5. (a) The toroidal magnetic field is ramped either up or down, moving the ICRF resonance toward or away from the center of the plasma. (b) The percentage of power inside the ITB radius changes with the resonance position, and the point where an ITB is either formed or lost is indicated.

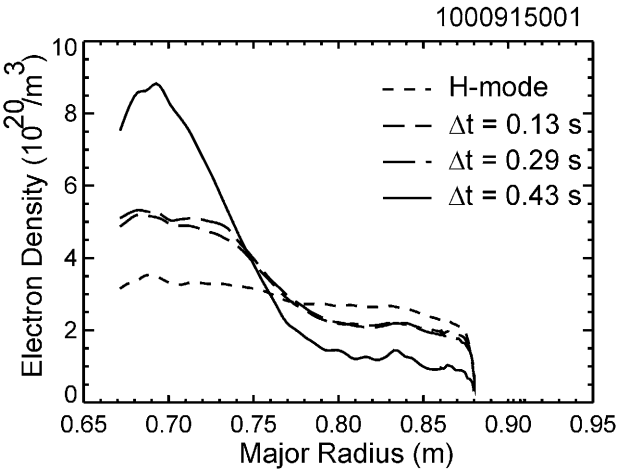

Fig. 6. Density profiles as an ITB develops in a purely ohmic EDA H-mode.

It should be noted that ITBs in C-Mod form only with q profiles (EFIT calculation) that increase monotonically from the center. Most observed ITBs exhibit sawteeth in the electron temperature, neutron rate, and soft x-ray emission throughout the life of the ITB, indicating that q_{min} is always less than 1 and located at the center. Also, the sawtooth inversion radius is typically $r/a = 0.15$, well inside the ITB foot location.

II.B. Ohmic H-Mode

The core density and pressure increase characteristic of ITB development occurs spontaneously in ohmic H-mode operation when an EDA H-mode is sustained for at least two energy confinement times. This suggests that the ITB formation is not triggered by the rf itself but is likely to result from a particular parametric profile. An example is shown in Fig. 6. The peaked density shown here arose spontaneously after the plasma went into H-mode. The ohmic H-mode is typically induced by ramping the toroidal magnetic field down to a low value in order to lower the H-mode threshold. Typically, the plasma sawtooth activity slows and stops as the density peaks, suggesting that q_0 exceeds 1 for at least part of this event. In this case the ITB lasted more than 400 ms, at least 10 energy confinement times, ending only as the plasma current began to ramp down in a controlled termination of the discharge. As in the off-axis ICRF-heated ITB, the central toroidal rotation is seen to decline as the ITB develops.

II.C. Pellet-Enhanced Performance

Transport barriers in the core plasma region were first reported following the injection of frozen hydrogen pellets into the Alcator C tokamak.[2,24] Strong central density peaking accompanied by a marked improvement in the energy confinement of the plasma was reported following the injection of both frozen hydrogen and deuterium pellets. It was observed that particle transport and thermal ion transport reduced to near-neoclassical levels.

On Alcator C-Mod, Li pellets (contributing typically 1×10^{20} electrons) have been injected in combination with on-axis ICRF heating to obtain the transport barrier associated with pellet-enhanced performance (PEP) mode.[25,26] The best results are obtained when the pellet is injected prior to the ICRF turn-on, so that the pellet can better reach the plasma center. The high density also enhances the focusing of the central ICRF deposition. As shown in Fig. 7, the PEP mode is characterized by a strong enhancement in the fusion neutron production, plasma stored energy, and central plasma pressure. The evolution of the density profiles is shown in Fig. 8 comparing the prepellet and postpellet profiles. The PEP mode is transient, in this case ending 0.11 s following the injections of the pellet.[15]

Imaging of the lithium pellet ablation trail has been used to measure the total magnetic field angle as the pellet traverses the plasma.[25] This information was used in conjunction with EFIT (Ref. 27) equilibrium reconstruction to obtain current density and q profile during PEP mode. The resulting q profile, measured 0.075 s after the pellet injection, 0.01 ms after the peak in the neutron production, was found to be hollow with $q_0 = 2$ and q_{min} slightly above 1 at $r/a = 0.4$. The current density profile is consistent with TRANSP calculations showing one-quarter of the current at $\rho = 0.3$, attributable to the bootstrap current for this case.

II.D. Enhanced Neutron Mode

The profile evolution shown in Fig. 9 is characteristic of the enhanced neutron mode, a short-lived ITB event

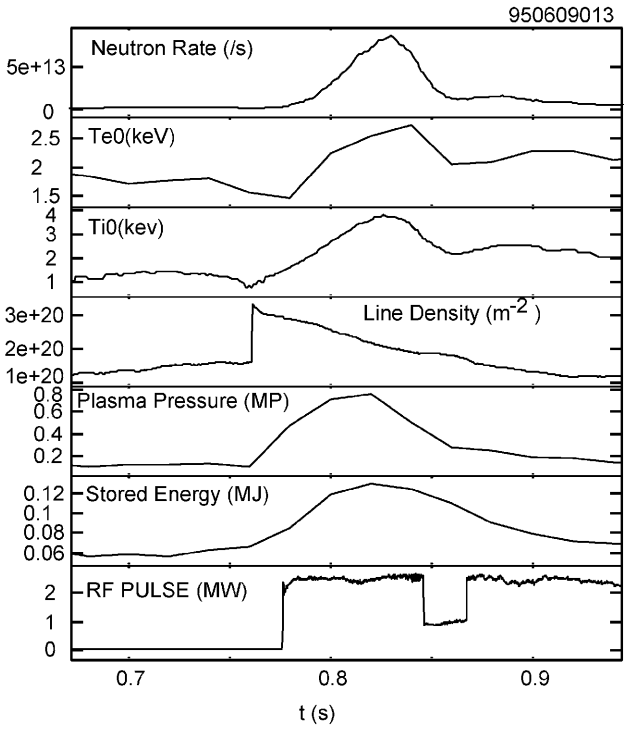

Fig. 7. Plasma parameters for a typical PEP mode shot. T_i0 is obtained by iteratively inverting the neutron rate using measured density profiles (adjusted for impurity depletion), assuming that the ion temperature profile is Gaussian of width similar to that of the electron temperature.

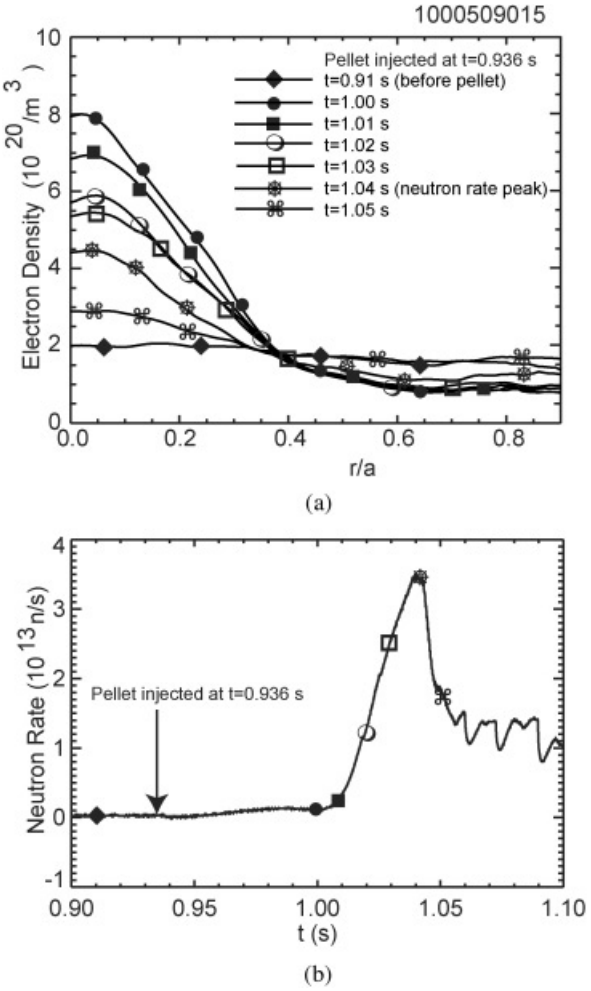

Fig. 8. (a) Density profiles and (b) global neutron rate for a PEP mode plasma. The peak in the neutron rate comes during the reheating of the plasma as the density is relaxing toward the prepellet value.

that occurs shortly after the plasma makes a transition from H- to L-mode. The profile shown here of the electron density n_e is derived from the profiles of the visible bremsstrahlung radiation,[21] corrected for temperature and Z_{eff} as in Sec. II.A.

The enhanced neutron mode is characterized by a large increase in the neutron rate, where increases of up to eight times have been observed. The usually flat density profile characteristic of H-mode plasmas, including an edge pedestal, immediately prior to the transition is shown in Fig. 9a. In short order, the density collapses in the outer region of the plasma while the central value is unchanged, temporarily resulting in a strongly peaked radial density distribution. The density in the outer part of the plasma flattens (Fig. 9b) while the central density remains peaked, indicating that a transport barrier has formed. During this time, the neutron production rate increases sharply (Fig. 9d), indicating that the central ion temperature is increasing, about 30% in this case (T_i is shown in Fig. 10). The enhanced neutron rate and ion temperature persist at an elevated level through several sawtooth cycles, even beyond the point when the central density collapses, reestablishing a flat L-mode density profile (Fig. 9c), which soon recovers to H-mode.

Enhanced neutron mode is seen following the majority of H- to L-mode transitions, in both ICRF and ohmic plasmas. Data from a typical Alcator C-Mod H- to L-mode transition are shown in Fig. 10. The global neutron rate is shown in the top trace, following the transition. It is indicative of an increase in the central ion temperature because the central density is steady and the line average density is decreasing. Ion temperature profile data on Alcator C-mod, obtained from a scannable array of five high–spectral resolution X-ray spectrometers[28] (HIREX), are typically measured with 0.1-s resolution, which is not sufficient to resolve these short-lived core barrier effects. However, by purposely triggering H- to L-mode transitions in similar discharges and averaging data for several pulses, the ion temperature profiles shown in Fig. 11 were obtained with 0.02-s resolution. The central ion temperature measured in this manner is higher following the end of the H-mode; however, the profile is not noticeably more peaked than the profile obtained in the H-mode phase. Gaussian fits to

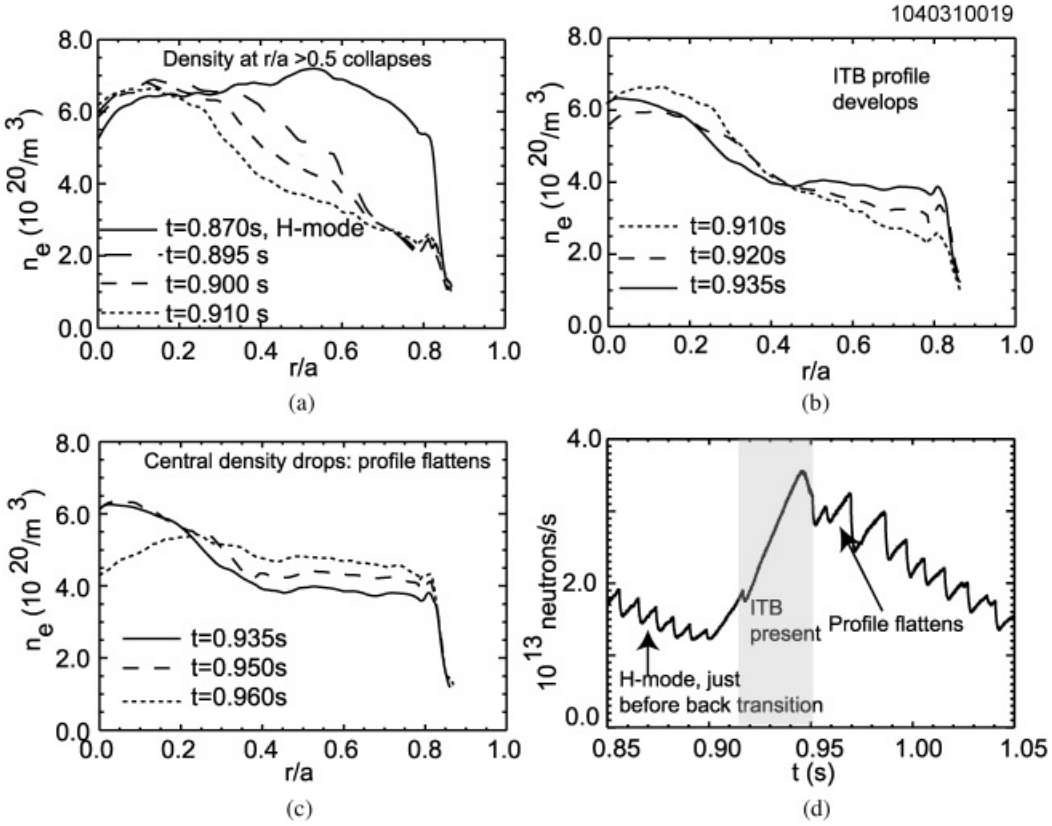

Fig. 9. (a) The density profile collapses at the H- to L-mode transition in enhanced neutron mode. (b) An ITB profile forms and (c) then returns to a flat profile. The neutron rate rises sharply during the ITB, then relaxes after the density profile once again becomes flat. Note that the neutron rate (i.e., ion temperature) relaxes more slowly than the density profile.

the data are included in the figure, and the $1/e$ width shows no significant change in either the ion or electron temperature profile.

Calculation of the scale length ratio η_x [defined as $d \ln T_x / d \ln n_x$ or L_n/L_T; $L_n = (1/n_x|dn_x/dr|)^{-1}$; $L_T = (1/T_x|dT_x/dr|)^{-1}$] shows that variation in this parameter results from changes in L_n. There are not sufficient ion temperature profile data to determine η_i for most of the data set, but η_e can be easily obtained from spatially resolved measurements of T_e obtained from electron cyclotron emission as well as from Thomson scattering. Because of the high-density operation in Alcator C-Mod, T_e and T_i are expected to be equal within the experimental error (typically 10% for the electron temperature, 12% for the central ion temperature derived from global neutron production, and 10 to 20% for HIREX profile data); it is assumed that the electron and ion temperature profiles are similar enough to use η_e as a surrogate for η_i, especially since the change in either quantity is entirely due to the change in density profile. η_e was calculated at the H- to L-mode transition for many events that showed the characteristic ITB formation, and it was found that η_e consistently drops to a value between 1 and 2 at the time that the neutron rate peaks, as in Fig. 12.

III. ITB CONTROL

III.A. Position Control

It is often not easy to tell from the experimental profiles at exactly what point in time and space an ITB has formed because the density peaking occurs over several energy confinement times. The profiles of density and/or temperature typically show a break in the slope where it can be inferred that the transport is different on either side of this position or ITB "foot." To determine this location, Tresset et al.[29] proposed using a dimensionless parameter ρ_T^*, defined to be the ratio of the Larmor radius at the ion sound speed (ρ_s) to the temperature gradient scale length $L_T(1/L_T = 1/T\, dT/dr)$, to locate the barrier. For the JET tokamak, a critical value of 0.014 is exceeded when an ITB is present in the core plasma. Other experiments such as the FTU tokamak[8] have found that the ITBs are well characterized by this parameter using the same critical value of 0.014. This parameter is in effect a proxy for the ratio of the $E \times B$ shearing rate to the maximum linear growth rate of the pressure gradient–driven modes.

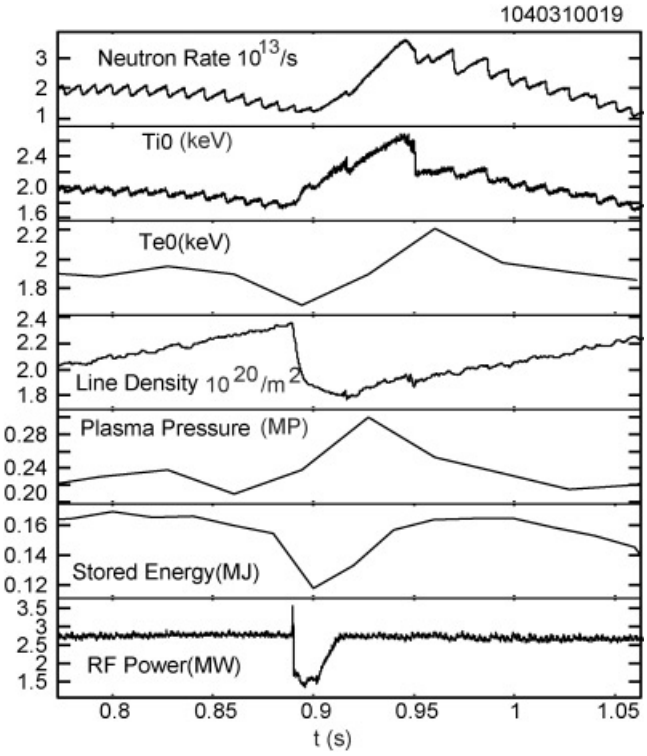

Fig. 10. Typical plasma parameters for an enhanced neutron mode. Along with the neutron rate increase, the central ion and electron temperatures increase while the line average density drops. The central plasma pressure increases, while there is a short-lived decrease in the plasma stored energy, which then recovers well before the plasma returns to H-mode.

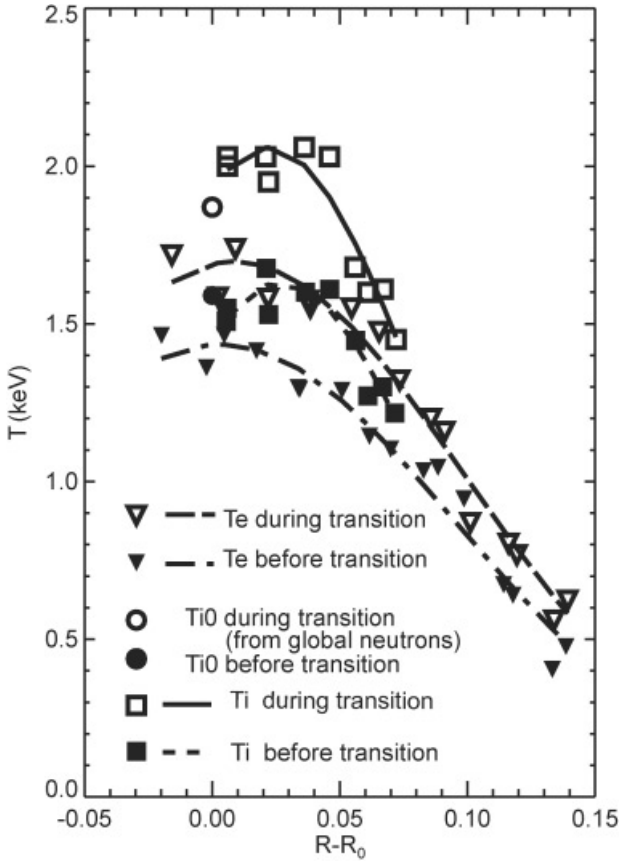

Fig. 11. Ion temperature and electron temperature profiles before and during the ITB phase of the enhanced neutron mode discharge. The temperatures increase, but the profile shape is maintained. Ion temperature has been averaged for three similar discharges to increase the signal and has an estimated 20% error.

On Alcator C-Mod, the break in slope indicating the presence of an ITB occurs in the density and pressure profiles and is usually not observable in the electron temperature profile. (Ion temperature profile data are not available.) It has been demonstrated that using a dimensionless parameter similar to the one for the JET tokamak, ρ_P^*, which is defined as ρ_s/L_P, where $1/L_p = 1/P\,dP/dr$, can be used to locate the ITB position in Alcator C-Mod (Ref. 18). Here it is plotted as a function of radius in Fig. 13a during the ITB phase of an Alcator C-Mod off-axis heated ITB plasma. It can be seen that although neither ρ_T^* nor $\rho_N^* = \rho_s/L_N$ exceeds the JET value of 0.014, ρ_P^*, which is the sum of the two, is higher than 0.014 in part of the core region of the plasma. Comparison of the location where ρ_P^* begins to exceed 0.014 to the position chosen for the ITB foot by an alternative method that calculates the derivatives of a functional fit to the data gives corresponding values for the location and onset time of the ITB. It should also be noted that at the point where $\rho_T^* = \rho_N^*$, the ratio of the density gradient scale length to the temperature gradient scale length (η_i) is equal to 1, and this location also tends to be near the barrier location (in the example shown in Fig. 13a, $\eta_i = 1$ at the same location that $\rho_P^* = 0.014$). Contours of ρ_P^* as a function of major radius and time are shown in Fig. 13b from the time of ITB onset. The position of the ITB foot determined from the density profile is shown as a heavy solid black line. It lies very close to the $\rho_P^* = 0.014$ contour.

The location of the ITB foot in Alcator C-Mod has been shown to narrow with increasing toroidal magnetic field.[19] Results found by scanning the plasma current with a fixed magnetic field suggested that the foot position moved outward with increasing current.[20] The current dependence has now been tested at high magnetic field as well, and the result from two field scans is shown in Fig. 14a. A clear trend with both increasing plasma current and decreasing magnetic field is demonstrated. Fitting the data with a power law to these quantities results in r/a at the foot position $\sim I_p^{0.94} B_t^{-1.13}$. Since the q profile of the plasma depends upon the ratio of these quantities, the data are also plotted as a function of q_{95} in

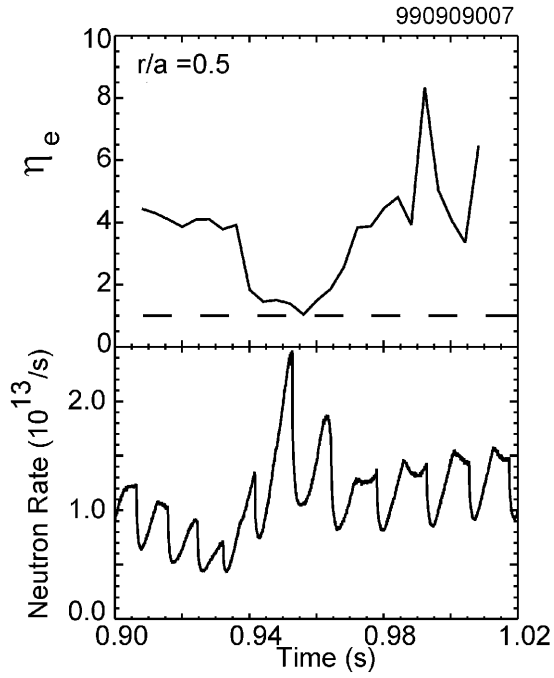

Fig. 12. The ratio of electron temperature scale length to electron density scale length decreases to a value near 1 at the plasma half-radius as the fusion neutron rate peaks in enhanced neutron mode plasmas. The enhanced neutron rate lasts for two to three sawtooth cycles, as can be seen from the sawtooth oscillations of the neutron output.

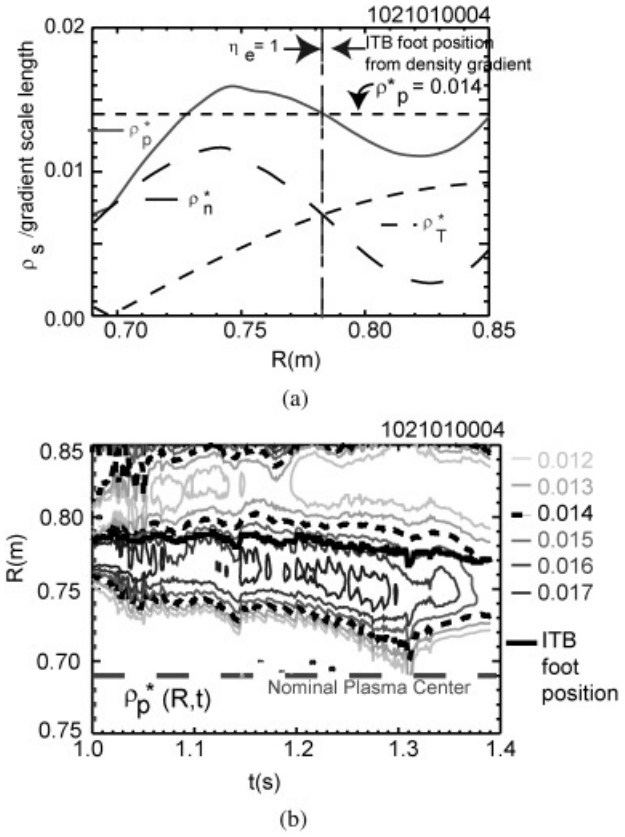

Fig. 13. (a) Dimensionless parameters ρ^*_T, ρ^*_N, and ρ^*_P as a function of radius when a typical ITB profile is present in the plasma. (b) Contours of ρ^*_p as a function of major radius and time.

Fig. 14b, showing a linear dependence of the ITB foot position with decreasing q_{95}. Comparison with the calculated q profile determined by EFIT shows that the typical ITB location lies between a q value of 1.1 and 1.34. (Note that these discharges are sawtoothing and that the sawtooth inversion radius is well determined to be inside the ITB foot location.)

III.B. Control of the Particle Accumulation

Typically, during the ITB phase of the Alcator C-Mod plasma, the particle and impurity influx is continuous

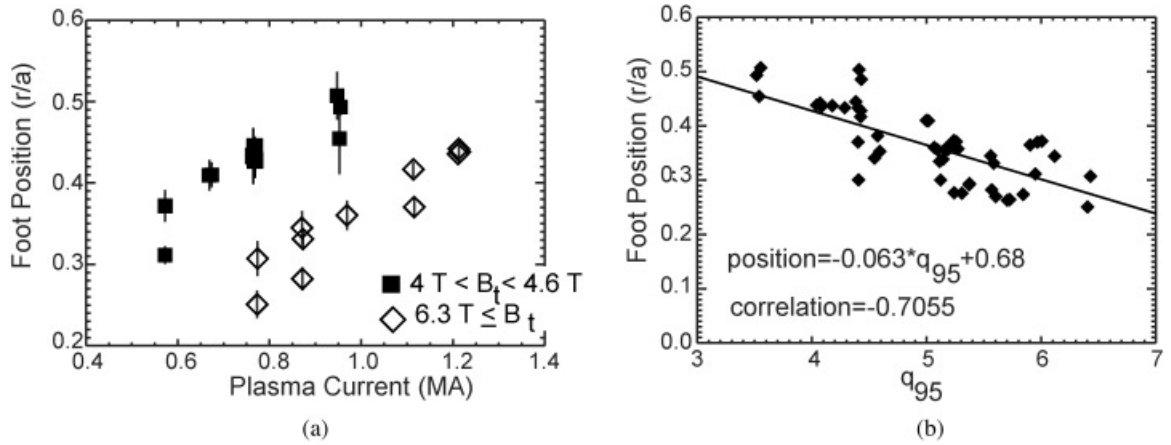

Fig. 14. The ITB foot position decreases with increasing toroidal magnetic field and decreasing plasma current.

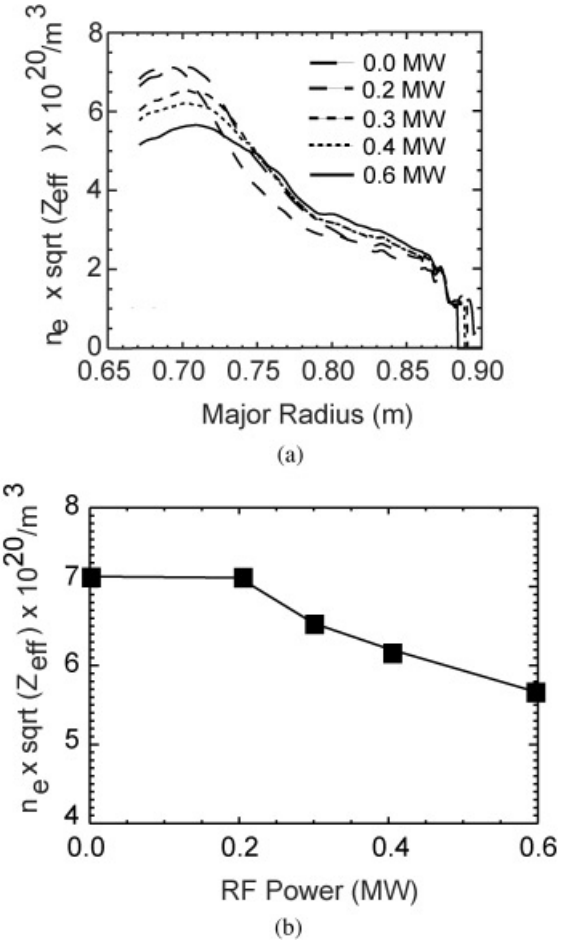

Fig. 15. Incremental central ICRF power is added to established ohmic H-mode ITBs over several shots: (a) density profiles and (b) final density decrease with increasing input power.

until either the current is brought down to end the discharge or the radiation level increases to the point where the plasma undergoes a back-transition to L-mode. It was demonstrated previously that this continued particle accumulation in the plasma core could be halted by the application of a small amount of central ICRF heating while preserving the ITB profile.[16,17] This has been demonstrated for ITBs created with off-axis ICRF heating as well as for those arising spontaneously from ohmic H-mode EDA conditions.[19]

An example of this effect is shown in Fig. 15. In this case similar ohmic EDA H-mode ITB plasmas were developed, and then central ICRF heating was turned on late in the discharge. This demonstrated that increasing levels of ICRF could be used to control how high the central density was allowed to rise before it was clamped. In this experiment and similar ones with off-axis ICRF heating, it was also found that there was an apparent relatively low power limit (~0.8 MW) to how much additional ICRF power could be added without degrading or destroying the ITB profile. More recently, ITB experiments that used a higher level of off-axis ICRF power have allowed a higher level of central ICRF power to be added while preserving the ITB. At this point, the central power that has been achieved appears to be limited only by the available source power, as long as the ratio of central to total power is maintained, as described in Sec. II.A.

Increasing the central power in this case resulted in strong central heating of the plasma and record plasma pressure for Alcator C-Mod. Exemplary plasma performance parameters have been achieved in this manner.[20] An example is shown in Fig. 16, with the electron pressure profiles shown in Fig. 17. The ITB was established with off-axis ICRF power of 2.3 MW. Once the ITB was fully formed, an additional 1.7 MW of central ICRF power was added. This caused a fivefold increase in the fusion production of the plasma, along with a near doubling of the electron and ion temperatures as well as the plasma

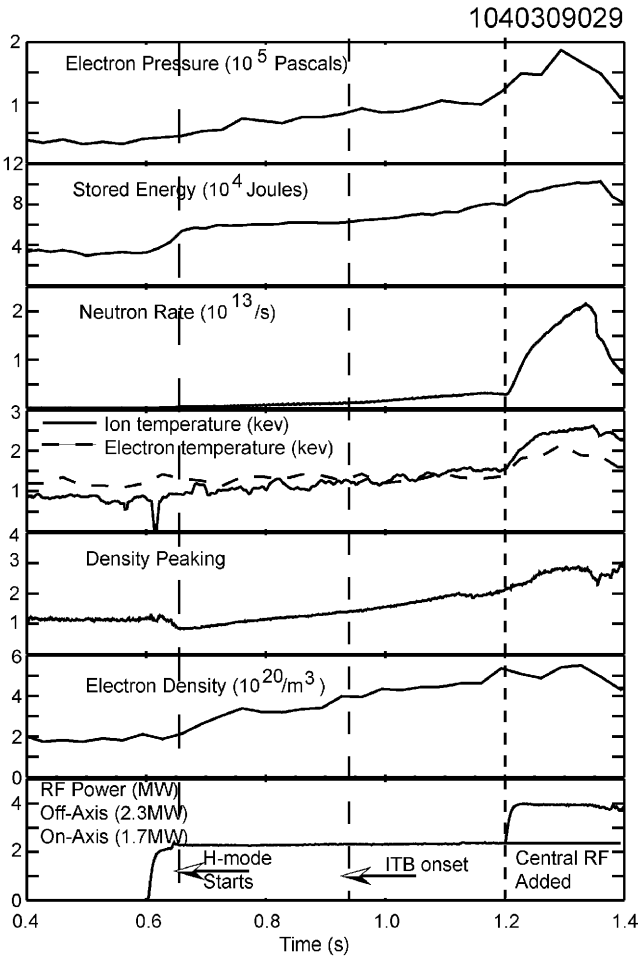

Fig. 16. Plasma parameters for a high-performance ITB discharge with added central ICRF power.

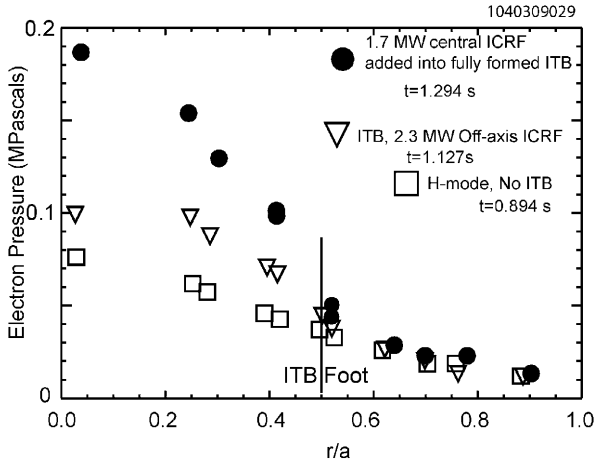

Fig. 17. Electron pressure profiles during the shot shown in Fig. 15. Strong pressure peaking is achieved with the addition of central ICRF.

pressure. No degradation of the density peaking occurred in this case.

IV. TRANSPORT ANALYSIS

The particle and thermal transport characteristics of the ITB discharges have been determined through use of the TRANSP code.[30] These calculations use the electron density and temperature profiles from the experiment and use a variable multiplier on χ_i (Chang and Hinton[31]) to obtain the ion temperature profiles consistent with the measured neutron rate. The central ion temperature for these plasmas is very close to the electron temperature, which makes separation of the ion and electron thermal transport channels impossible due to the uncertainty in the exchange term. Thus, the behavior of an effective thermal transport coefficient,

$$\chi_{eff} \equiv \frac{n_e \chi_e \nabla T_e + n_i \chi_i \nabla T_i}{n_e \nabla T_e + n_i \nabla T_i} \quad ,$$

is reported here. As the ITB develops in these plasmas, the value of χ_{eff} in the core region decreases from the typical H-mode value of 1.1 to 1.4 m^2/s to 0.1 to 0.2 m^2/s, which is equivalent to the value of neoclassical ion thermal transport for these plasmas. This is shown in Fig. 18 for both off-axis ICRF-heated and ohmic H-mode ITB plasmas.

These plasmas often have sawtooth instability present throughout the development of the ITB. This allows use of the propagation rate of the heat pulse that occurs at the sawtooth crash to investigate further the thermal transport in these plasmas. A significant delay in the propagation of this heat pulse across the transport barrier regions

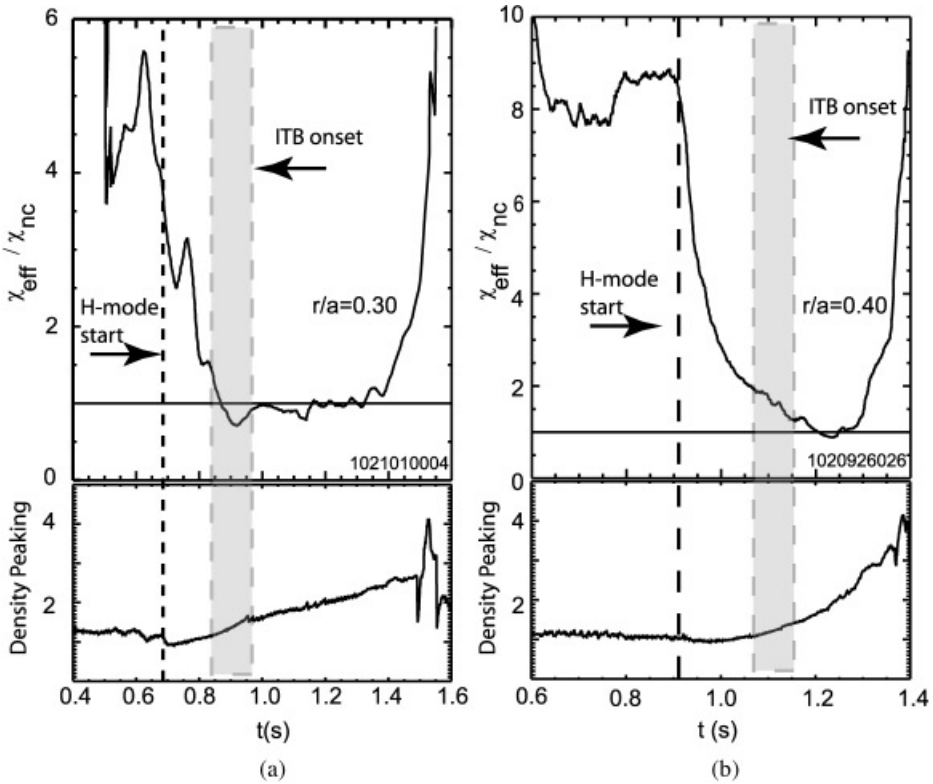

Fig. 18. χ_{eff} in the core region decreases to the neoclassical ion thermal transport during an ITB for both (a) off-axis ICRF-heated and (b) ohmic H-mode ITB plasmas.

has been reported[17] in the soft X-ray emission from what is observed during H-mode, as can be seen in Fig. 19. This delay is best modeled by using a narrow region (<0.02 m) of reduced electron heat transport at or near the location of the ITB foot, determined from the electron density profile. This has been interpreted as a decrease in the incremental electron heat conductivity to a value of approximately 0.1 m^2/s at the barrier, consistent with the typical χ_{eff} determined by TRANSP calculation.

It is also noted that the particle diffusivity decreases as an ITB develops to a level similar to that of χ_{eff} in the core region.[32] This decrease in the outward particle diffusion allows the inward neoclassical pinch term to dominate the transport. The pinch term is sufficient to account for the experimentally observed central density increase.[32,33] The neoclassical pinch velocity is relatively large in Alcator C-Mod because the device is small compared to other tokamaks of this generation, resulting in a larger toroidal electric field. It also operates at somewhat lower electron temperature, which further contributes to the pinch velocity. The impurity diffusion coefficient and velocity also tend toward neoclassical values during the ITB phase of the plasma.

The bootstrap current inside the barrier region increases by as much as 10 times as the ITB develops and reaches a local value that is 10 to 12% of the ohmically induced current. These values of ITB-generated bootstrap current are obtained in both ohmic EDA H-mode plasmas as well as for off-axis ICRF-generated ITBs (Refs. 16 and 19).

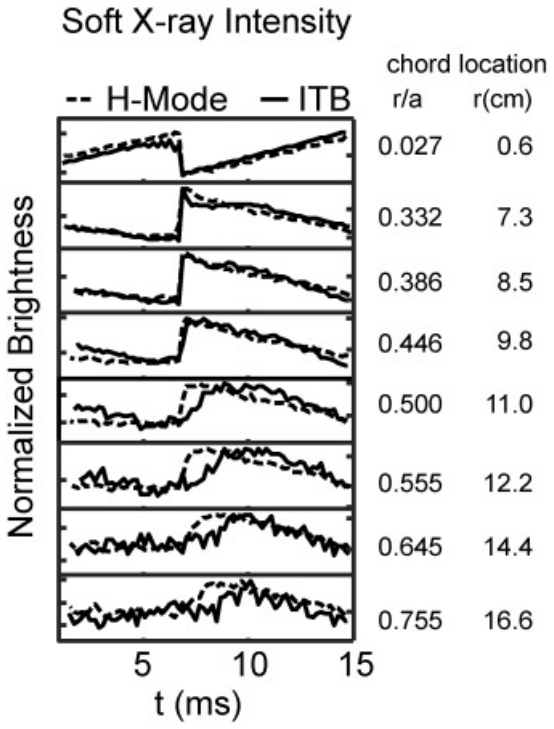

Fig. 19. During an ITB, the heat pulse resulting from a sawtooth crash is delayed in its propagation from what is seen during H-mode.

V. GYROKINETIC SIMULATIONS AND ANALYSIS

Ion thermal transport for typical Alcator C-Mod H-mode plasmas is thought to be dominated by turbulence resulting from ITG-driven modes.[34] The formation of a transport barrier in the plasma is believed to result from the reduction of this turbulent transport at the barrier and in the core. The reduced particle transport allows the neoclassical particle pinch to steadily peak the density profile for a duration lasting tens of energy confinement times.

Exploration of the drift wave stability in C-Mod ITB plasmas has been done using the GS2 code,[35,36] which treats the gyrokinetic Vlasov-Maxwell equations as an initial value problem. Linear stability at the onset of the ITB has been explored in depth,[32,37,38] including mapping the evolution of the ITB trajectory through stability space.[32] Full nonlinear modeling has been carried out for specific off-axis heated ITB cases that received supplemental central heating as a control mechanism.[32,38]

At the onset time for the ITB, the barrier region is found to be marginally stable or stable to long-wavelength toroidal ITG modes.[32,37,38] The addition of off-axis heating broadens the temperature profile, stabilizing ITG modes.[38] The evolution of the maximum linear growth rate at the position $\rho = 0.4$ just inside the ITB foot location, where ρ is the square root of the normalized toroidal flux ($\rho \sim r/a$), is shown in Fig. 20, along with the inverse density scale lengths and temperature.[32,38] It can be seen that at this position, which lies just to the inside of the ITB foot, the density gradient scale length is steadily decreasing after the onset of the EDA H-mode, which occurs just before $t = 0.8$ s. The temperature gradient is just below marginal stability for toroidal ITG modes at the time of ITB onset. The ITG mode is strongly growing outside the barrier, where the density gradient is relatively flat, however. In this case, after $t = 1.0$ s, when the ITB is fully established and the density scale length at $\rho = 0.4$ is no longer decreasing, the maximum linear growth rate becomes dominated by the TEM, which is driven by the steep density gradient. The sign of the real frequency changes from the ion to the electron direction at this time. The mode disappears when an adiabatic electron response is used. Considering these indications, together with the insensitivity of the mode to the temperature gradient, confirms that the dominant instability has changed from ITG to TEM.

The peaking of the plasma density occurs when the core turbulent transport found in the nonlinear simulation declines and the particle diffusivity decreases to a value near that of the effective heat diffusivity χ_{eff}

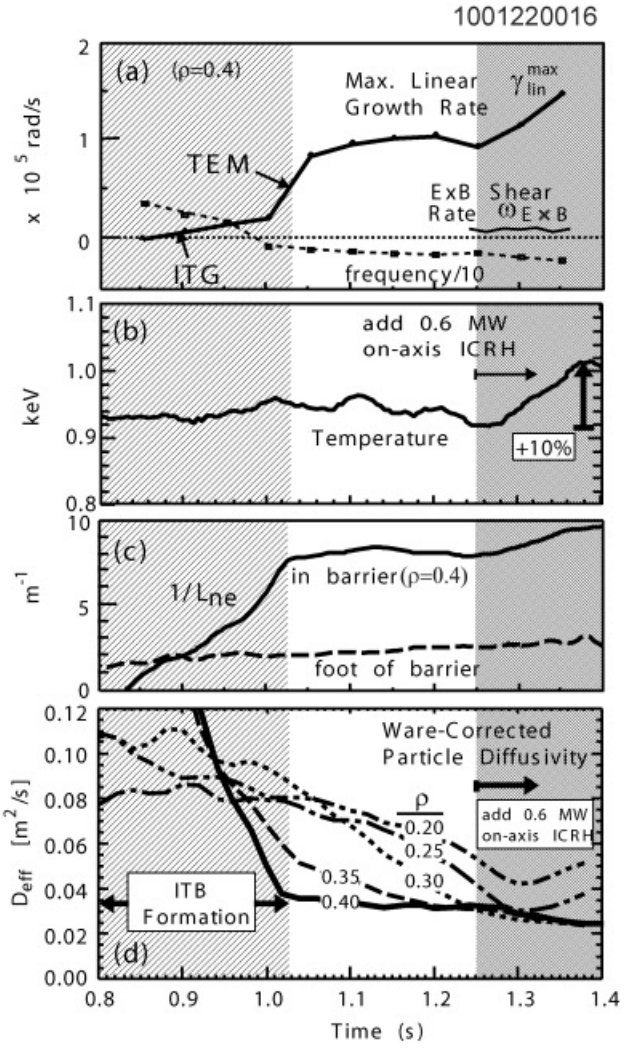

Fig. 20. Temporal evolution of (a) maximum linear growth rate, radial electric field shearing rate, and real frequency at the ITB radius ($\rho = 0.4$), (b) temperature at the ITB radius, (c) inverse density gradient scale length from visible bremsstrahlung data, and (d) effective particle diffusivity inside the ITB foot, from density profile measurements and calculated Ware pinch.

(Ref. 32). The neoclassical (or Ware) pinch velocity is sufficiently strong in Alcator C-Mod to account for the central peaking of the density without requiring any anomalous pinch. This is evidenced by the observation that the particle diffusivity inferred from the continuity equation, using the calculated neoclassical pinch, remains positive for all time.[32] Accordingly, the nonlinear gyrokinetic simulations for the flat density gradient case, corresponding to early times, show an insignificant anomalous turbulent particle pinch, several orders of magnitude less than the Ware pinch.[32] As the density gradient increases, the turbulent particle flux changes from inward to outward.

The increasing density profile gradient is further stabilizing to toroidal ITG-driven modes but at the same time is destabilizing to TEMs in the barrier region. The turbulent diffusivity from the TEM was found to increase with temperature in the gyro-Bohm manner, $D_e \propto T_e^{3/2}$ (Ref. 32), with a weak departure due to collisionality effects. Thus, even a small increase in the central power, as occurs with even a few hundred kilowatts of on-axis ICRF, can contribute enough additional heating to cause the TEM-driven turbulent transport inside the barrier to balance the influx from the neoclassical pinch, which decreases with temperature. The balance between the collisional inflow and turbulent outflow results in a stable equilibrium.[32] The nonlinear gyrokinetic simulations of the TEM turbulence in this late quasi-steady phase reproduce the particle and energy fluxes inferred from transport analysis within measurement error, as shown in Fig. 21. This supports the picture that increased TEM turbulent outflow accompanies the addition of central ICRF power, which halts the density rise. The means of controlling the particle and impurity influx can be inferred from the temperature sensitivity of the equilibrium, revealed in the simulations.[32]

Recently obtained results from phase-contrast imaging (PCI) measurements have shown the existence of fluctuations in the density that appear to increase in intensity with the addition of central ICRF power into an ITB plasma.[38] The wave number and frequency are found to be consistent with the spectrum observed in the nonlinear turbulence simulations of one of these plasmas, although the PCI measurement cannot yet establish localization of this oscillation.[39] The relative increase in fluctuation intensity during on-axis heating is in close agreement with the simulations,[38] however. Core fluctuations that appear to intensify with increasing density gradient during ITB plasmas have been reported from measurements using a heterodyne electron-cyclotron-emission diagnostic.[40]

Several observations regarding the formation of the ITB are not yet understood. The slowing and sometime reversal of the central plasma rotation as the plasma density becomes more peaked suggests that rotational shear may play a role. However, initially the ITB profile begins to build up when the plasma is in H-mode. The apparent velocity profiles at that time are typically flat (no velocity shear), from $0 < r/a < 0.6$ (Refs. 41 and 42), slightly outside of the ITB foot position $r/a \approx 0.45$ during the H-mode. The central velocity has been observed to decrease slightly earlier than that at larger radii during the ITB (Refs. 41 and 42), an effect that needs to be studied in more detail when greater radial resolution in the measurement becomes available.

VI. DISCUSSION AND FUTURE WORK

The ITBs observed in Alcator C-Mod form spontaneously in the pressure profiles in EDA H-mode plasmas

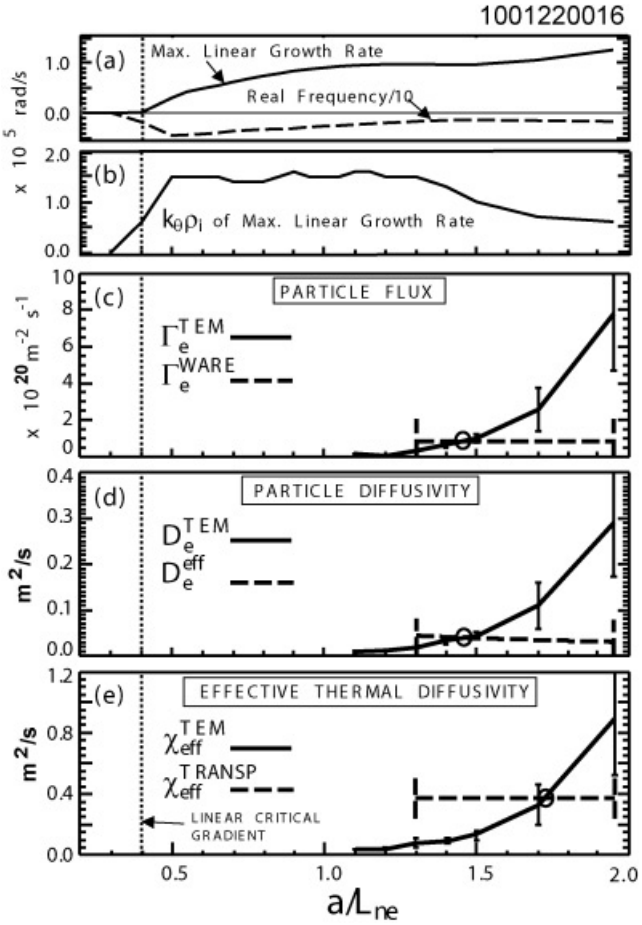

Fig. 21. Comparison of simulated and measured transport, at $\rho = 0.4$, $t = 1.2$ s (error bars take into account the effects of uncertainty in L_{ne} from possible Z_{eff} gradients) as functions of a/L_{ne} from linear GS2 simulations: (a) maximum growth rate and real frequency; (b) poloidal wave number $k_\theta \rho_i$ yielding the maximum linear growth rate; (c) particle flux and (d) particle diffusivity from TEM turbulence, equaling that from the Ware pinch for $a/L_{ne} = 1.47$; and (e) effective thermal diffusivity, matching the TRANSP value at $1/L_{ne} = 1.72$, all within experimental error.

if the input power profile is broadly distributed across the plasma rather than centrally peaked. Short-lived ITBs appear at the back-transition from H- to L-mode as well as following pellet injection in ICRF-heated plasmas. Except in the case of pellet injection, these are formed in the absence of additional particle or momentum sources in the plasma. While the long-lived ITBs have been seen only in EDA H-modes, it is thought that the relevant parameter is the steadiness of the H-mode (edge-localized mode–free H-modes tend to have frequent back-transitions in Alcator C-Mod) and that it has to last long enough for the neoclassical pinch velocity to peak the central density. Once the central density and impurities begin to peak, they will generally continue to rise until the H-mode collapses.

It has been demonstrated, however, that the addition of central ICRF power into an established ITB plasma will control the further rise of the central particle and impurity accumulation, likely through amplifying the TEM-driven turbulent transport. A bonus of this process is the increase in the central temperature, pressure, and fusion rate in the core. Near-doubling of the central temperature and pressure (to 0.2 MPa) and fivefold increase in the fusion rate have been achieved. The experimental program plans include maximizing the power input into these plasmas to determine if there is a limit to the central pressure that can be obtained and the nature of these limits.

Transport analysis and gyrokinetic stability modeling have demonstrated that the target plasmas exhibit a reduction of turbulent transport in the region lying inside the ITB foot, which allows the neoclassical pinch to dominate the particle flow and allows the density to peak up. Eventually, the steepening of the density profile turns on increasing TEM-driven transport, which eventually balances the effects of the neoclassical pinch. Since the diffusivity has been shown to scale in a gyro-Bohm fashion with a $T_e^{3/2}$ dependence, the increase in temperature associated with the addition of central power leads to balanced flow and steady-state density profiles.

The ITB foot location has been determined to depend on increasing plasma current and decreasing toroidal magnetic field, making it likely that the functional dependence is on the safety factor or on the magnetic shear. Determination of the nature of this dependence is the subject of ongoing work in gyrokinetic stability modeling of these plasmas. It will also be explored experimentally when lower-hybrid current drive becomes available, allowing specific tailoring of the q profile. It is expected that measurements of the q profile will soon be available as well.

The current program of research in C-Mod ITBs involves study of the role of critical temperature gradient, density profile, rotational shear, and magnetic shear in the ITB onset. This program is being pursued both with the available experimental tools as well as in theory and modeling using the GS2 code. The role of density fluctuations will be explored with improved resolution of the PCI and reflectometry diagnostics in the short term. The PCI diagnostic has been upgraded to allow the fluctuation measurement to be spatially located within the plasma.

The Alcator C-Mod program will soon begin operation of lower-hybrid wave current drive (LHCD) experiments. This will allow further exploration of the effects of tailoring of the q profile on the ITB foot position. It will also provide information on the role of the neoclassical pinch in establishment of these ITBs, since this pinch is driven by the toroidal electric field, which can be minimized or eliminated in LHCD experiments.

ACKNOWLEDGMENTS

This work is supported by U.S. Department of Energy Cooperative Agreement DE-FC02-99ER54512. The authors would like to thank A. Hubbard (Massachusetts Institute of Technology), A. Lynn (University of Nevada), and P. Phillips (University of Texas at Austin, Fusion Research Center) for high-resolution electron temperature data and D. Mossessian and J. Hughes for Thomson scattering density and pressure profiles. They would also like to thank S. Wolfe, J. Snipes, B. Granetz, R. Parker, B. Rowan, and J. Irby for their expert operation of the tokamak for many of the experiments presented here, Y. Lin for operation of the ICRF system, and the Alcator C-Mod Operations Group for their support of this work.

REFERENCES

1. ASDEX TEAM, *Nucl. Fusion*, **29**, 1959 (1989).
2. M. J. GREENWALD et al., *Phys. Rev. Lett*., **53**, 352 (1984).
3. F. M. LEVINTON et al., *Phys. Rev. Lett*., **75**, 4417 (1995).
4. E. J. STRAIT et al., *Phys. Rev. Lett*., **75**, 4421 (1995).
5. T. FUJITA et al., *Phys. Rev. Lett*., **78**, 2377 (1997).
6. O. GRUBER et al., *Phys. Rev. Lett*., **83**, 1787 (1999).
7. Y. KOIDE et al., *Phys. Rev. Lett*., **72**, 3662 (1994).
8. V. PERICOLI RIDOLFINI et al., *Nucl. Fusion*, **6**, 469 (2003).
9. A. FUJISAWA et al., *Phys. Rev. Lett*., **82**, 2669 (1999).
10. B. LEBLANC et al., *Phys. Plasmas*, **2**, 741 (1995).
11. S. I. LASHKUL et al., *Plasma Phys. Control. Fusion*, **42**, A169 (2000)
12. R. C. WOLF, *Plasma Phys. Control. Fusion*, **45**, R1 (2003).
13. J. W. CONNOR et al., *Nucl. Fusion*, **44**, R1 (2004).
14. J. E. RICE et al., *Nucl. Fusion*, **41**, 277 (2001).
15. C. L. FIORE et al., *Phys. Plasmas*, **8**, 2023 (2001).
16. J. E. RICE et al., *Nucl. Fusion*, **42**, 510 (2002).
17. S. J. WUKITCH et al., *Phys. Plasmas*, **9**, 2149 (2002).
18. J. E. RICE et al., *Nucl. Fusion*, **43**, 781 (2003).
19. C. L. FIORE et al., *Phys. Plasmas*, **10**, 2480 (2004).
20. C. L. FIORE et al., *Plasma Phys. Control. Fusion*, **46**, B281 (2004).
21. E. S. MARMAR et al., *Rev. Sci. Instrum*., **72**, 940 (2001).
22. J. E. RICE et al., *Nucl. Fusion*, **39**, 1175 (1999).
23. M. BRAMBILLA, *Plasma Phys. Control. Fusion*, **41**, 1 (1999).
24. S. M. WOLFE et al., *Nucl. Fusion*, **26**, 219 (1986).
25. D. T. GARNIER et al., *Proc. 16th Int. Conf. Fusion Energy*, Montreal, Canada, Vol. 1, p. 90, International Atomic Energy Agency (1997).
26. Y. TAKASE et al., "Radiofrequency-Heated Enhanced Confinement Modes in the Alcator C-Mod Tokamak," *Phys. Plasmas*, **4**, 1647 (1997).
27. L. LAO et al., *Nucl. Fusion*, **25**, 1611 (1985).
28. J. E. RICE and E. S. MARMAR, *Rev. Sci. Instrum*., **66**, 752 (1995).
29. G. TRESSET et al., *Nucl. Fusion*, **42**, 520, (2002).
30. R. HAWRYLUK, in *Physics of Plasma Close to Thermonuclear Conditions*, Vol. I, Commission of the European Communities, Brussels (1979).
31. C. S. CHANG and F. L. HINTON, *Phys. Fluids*, **25**, 1493 (1982).
32. D. R. ERNST et al., *Phys. Plasmas*, **10**, 2637 (2004).
33. P. T. BONOLI et al., *Bull. Am. Phys. Soc*., **46**, 54 (2001).
34. M. J. GREENWALD et al., *Nucl. Fusion*, **37**, 793 (1997).
35. M. KOTSCHENREUTHER et al., *Comput. Phys. Commun*., **88**, 129 (1995).
36. W. DORLAND et al., *Phys. Rev. Lett*., **85**, 5579 (2000).
37. M. H. REDI et al., *Phys. Plasmas*, **12**, 072519-1 (2005).
38. D. R. ERNST et al., *Proc. 20th IAEA Fusion Energy Conf.*, Vilamoura, Portugal, TH/4-1, International Atomic Energy Agency (2004); available on the Internet at http://www.naweb.iaea.org.napc/physics/fec/fec2004/datasets/th4-1.html.
39. N. P. BASSE et al., *Phys. Plasmas*, **12**, 052512 (2005).
40. A. G. LYNN et al., "Observations of Core Modes During RF-Generated Internal Transport Barriers in Alcator C-Mod," *Plasma Phys. Control. Fusion*, **46**, A61 (2004).
41. W. D. LEE et al., *Phys Rev. Lett*., **91**, 205003 (2003).
42. J. E. RICE et al., *Nucl. Fusion*, **44**, 379 (2004).